TRPIV measurement of turbulent coherent structures in a drag-reducing flow by polymers

Xinlei Guan,[1, a)] Nan Jiang,[1, 2, 3, 4, b)] Lu Cheng,[1] and Hao Zhang[1]

[1)] *Department of Mechanics, Tianjin University, Tianjin 300072, China*
[2)] *Tianjin Key Laboratory of Modern Engineering Mechanics, Tianjin 300072, China*
[3)] *State Key Laboratory of Nonlinear Mechanics, Institute of Mechanics, Chinese Academy of Sciences, Beijing 100190, China*
[4)] *Nankai University–Tianjin University Center for LiuHui Applied Mathematics Tianjin 300072, China*

(Received 28 June 2013; accepted 29 June 2013; published online 10 July 2013)

Abstract Fully developed turbulent flow fields with and without polymer solution at the same Reynolds number were measured by time-resolved particle image velocimetry (TRPIV) in a water channel to investigate the mechanism of drag-reducing solution from the view of coherent structures manipulation. The streamwise mean velocity and Reynolds stress profiles in the solution were compared with those in water. After adding the polymer solution, the Reynolds stress in the near-wall area decreases significantly. The result relates tightly to the decease of the coherent structures' bursting. The spatial topology of coherent structures during bursts has been extracted by the new mu-level criterion based on locally averaged velocity structure function. The effect of polymers on turbulent coherent structures mainly reflects in the intensity, not in the shape. In the solution, it is by suppressing the coherent structures that the wall friction is reduced. © *2013 The Chinese Society of Theoretical and Applied Mechanics.* [doi:10.1063/2.1304206]

Keywords spatial topology of coherent structures, turbulent drag-reducing flow, polymer additives, TRPIV

Since Toms[1] discovered the phenomenon that dramatic drag reduction occurred in turbulent wall-bounded flow after dissolving a small amount of long-chain, high-molecular weight polymers, it has drawn much attention afterwards because of the increasing importance of drag reduction in modern fluid engineering application. However the mechanism of polymers reducing drag is still not fully understood by scientists. During the past sixty years, many researches were performed experimentally on polymeric drag reduction. Early researchers[2,3] focused on the effects of polymers on the time-averaged turbulence statistics. They found out that there was an asymptotic value for the maximum drag reduction and the buffer region played an important role in drag-reducing flows. Then, coherent turbulent boundary layer structure research initiated by Kline et al.[4] impelled the research on drag-reduction. Luchik and Tiederman[5] employed mu-level method on the coherent structures in turbulent channel flows for the laser Doppler velocimetry (LDV) dataset to discuss how polymers affect the bursting frequency, Reynolds stress, and streak spacing. However, as a sort of traditional conditional sampling method, the method they used has some limitations. More recently, Motozawa et al.[6] presented channel flow experimental investigation with polymer solution injection, using particle image velocimetry (PIV). They showed polymer solution weakened the intensity and frequency of ejections and sweeps in the near-wall region. Regretfully they did not extract the spatial topologies of coherent structures.

In the present paper, a new mu-level method will be applied to investigate the mechanism of drag reduction by polymer additives from the view of coherent structure manipulation. The new mu-level is created on the basis of locally averaged velocity structure function which was proposed by Jiang et al.[7–9] to overcome the two main shortcomings of the traditional conditional sampling method. One is the subjectivity due to the preselected threshold and the other is that small-scale fluctuation might affect the detection results. This kind velocity structure function represents the local deformation and relative motion of turbulent eddy structures within definite scale. One-dimensional locally averaged velocity structure function is given by

$$\delta u_x\left(x_0, l_x; y\right) = \overline{u\left(x, y\right)}_{x\in[x_0, x_0+l_x]} - \overline{u\left(x, y\right)}_{x\in[x_0-l_x, x_0]}, \tag{1}$$

where l_x is the spatial scale along the streamwise.

The mu-level method looks for the deficit from the mean streamwise velocity component and identifies an event when low-speed fluid ejects through the detection point. In this case, the local streamwise fluctuating velocity reaches the negative minimum instantaneously. And meanwhile, the low-pass filtered first derivative reaches the zero point from negative to positive. Correspondingly, for the case of high velocity fluid inrushing toward the wall, the low-pass filtered first derivative reaches the zero point from positive to negative. Thus the new mu-level method of identifying coherent structures near the wall based on the locally averaged

[a)] Email: guan_xinlei@126.com.
[b)] Corresponding author. Email: nanj@tju.edu.cn.

velocity structure function is given by

$$D(x_0, l_x; y_0) = \begin{cases} 1 \text{ (ejection)}, \\ \quad \text{if } \delta u_x(x_0 - \Delta x, l_x; y_0) < 0 \\ \quad \text{and } \delta u_x(x_0 + \Delta x, l_x; y_0) > 0, \\ -1 \text{ (sweep)}, \\ \quad \text{if } \delta u_x(x_0 - \Delta x, l_x; y_0) > 0 \\ \quad \text{and } \delta u_x(x_0 + \Delta x, l_x; y_0) < 0, \\ 0, \quad \text{otherwise}, \end{cases} \tag{2}$$

where Δx is the grid size in the streamwise direction.

This present experiment was conducted in a recirculating water channelof Tianjin University. The water-channel system had a working section 1 200 mm long, 140 mm wide, and 150 mm deep. On the bottom surface of the channel, a flat acrylic glass plate with a 4:1 elliptical leading edge was horizontally mounted to be utilized as a test surface. The plate dimensions are 1 050 mm × 138 mm × 10 mm. The turbulent flow developed along the plane was tripped by a trip wire on the leading edge at a free-stream velocity of 0.18 m/s. The freestream velocity and boundary determine the Reynolds number. The PIV system was composed of a double-pulse laser, a CCD camera, a synchronizer, and a computer set up with image-processing software (Dantec, Dynamics Studio ver. 3.20.0). The laser sheet with a thickness of about 0.8 mm was oriented in the x–y plane 0.9 m downstream of the leading edge. Hollow glass microspheres with the median diameter of 10 μm and a density of 1.03 g/cm^3 were used as tracer particles. The synchronization device communicated with the computer, which generated pulses to control the double-pulse laser, and the CCD camera having a resolution of 1 280 × 1 025 pixels. It recorded 6 400 snapshots of particle images for each turbulent flow with and without polymer solution at the sampling frequency of 600 Hz. The following steps were applied to analyze the PIV images. (1) Adaptive correlation was carried out with interrogation windows of 32 × 32 pixels and an overlap rate of 75%. (2) Range validation was applied to remove the noise from manufactured velocity vector fields. (3) Average filter was employed to filter out vector maps by arithmetic averaging over vector neighbors with typical averaging area size of 3×3 vectors. Each flow field consisted of 157 × 125 two-dimensional velocity vectors. The field was about 90.71 mm × 72.55 mm. The drag-reducing additive was an aqueous solution of analytically pure polyacrylamide (PAM) having a molecular weight of 5 million. From the results reported by Kenis,[10] the polyacrylamide has a good anti-shear performance compared with other commonly used polymers, such as polyethylene oxide (PEO). With this polymer solid dissolved in water, the polymer solution were initially mixed to 16.6 × 10^3 based on weight calculation. After the polymer being added to solution, it was stirred gently for duration of a few hours. Then, this concentrated mixture was diluted to 0.19 × 10^{-3} in a tank with dials and allowed to hydrate for hours

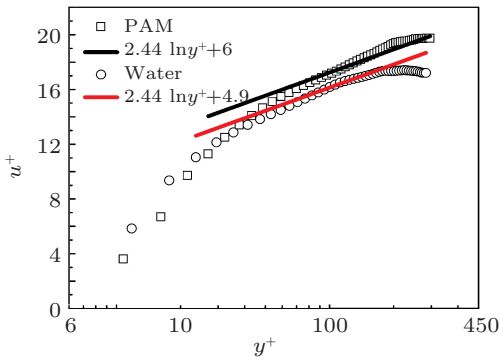

Fig. 1. Streamwise mean velocity profiles of turbulent boundary layer.

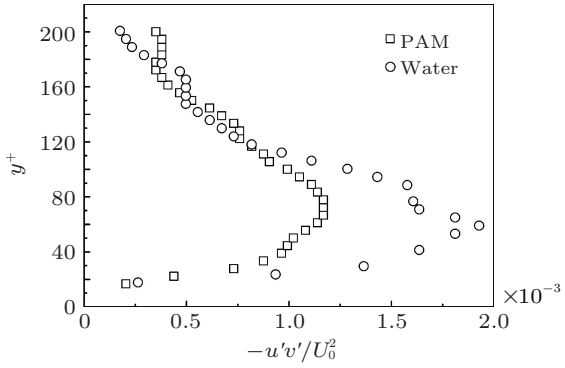

Fig. 2. Reynolds stress distribution in wall-normal direction.

before using. The dynamic viscosity of the solution was 1.06 mPa·s, and that of water was 1.01 mPa·s.

Figure 1 compares the mean streamwise velocity profiles for the water flow and the drag reducing flow that matches Reynolds number of the water flow. The log-law profile of streamwise velocity is expressed as $u^+ = A \ln y^+ + B$, in which $u^+ = u/u_*$ and $y^+ = yu_*/\nu$. The "+" superscript indicates that variable was normalized by the friction velocity and the kinematic viscosity. According to the equations above, the Newton iterative and steepest descent method which introduced in Ref. 11 are used to calculate A, B and friction velocity. Compared with the case for water the friction velocity appears smaller for drag-reducing solution as well as the thickening of turbulent boundary layer, and the ratio of drag reduction is 16.58%. The measured mean velocity profiles, no matter with or without polymers, shown in Fig. 1 are both in agreement with the log-law. It is noted that in the solution, the value of B appears larger compared with that in the water. The reason for this is that the logarithmic sublayer is lifted from the wall and the buffer sublayer becomes thicker[12] after adding the polymer solution. The effect reflects the reduction of the frictiondrag of the wall turbulence.

The profiles of Reynolds stress non-dimensionalized with the mean velocity square for the solution and water are shown in Fig. 2. In water flow, Reynolds stress has a distinguished peak near the wall. In contrast the peak

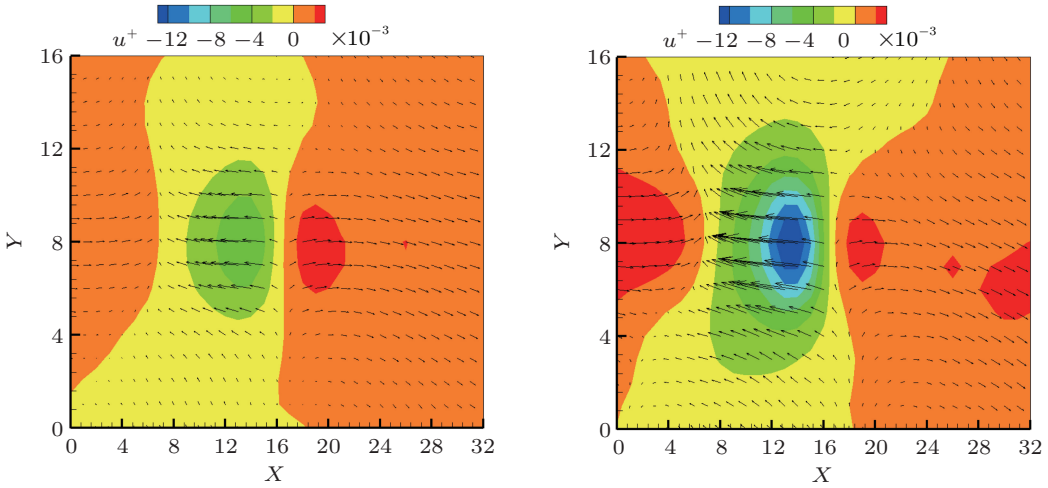

(a) PAM (b) Water

Fig. 3. Contours of streamwise fluctuating velocity during ejection.

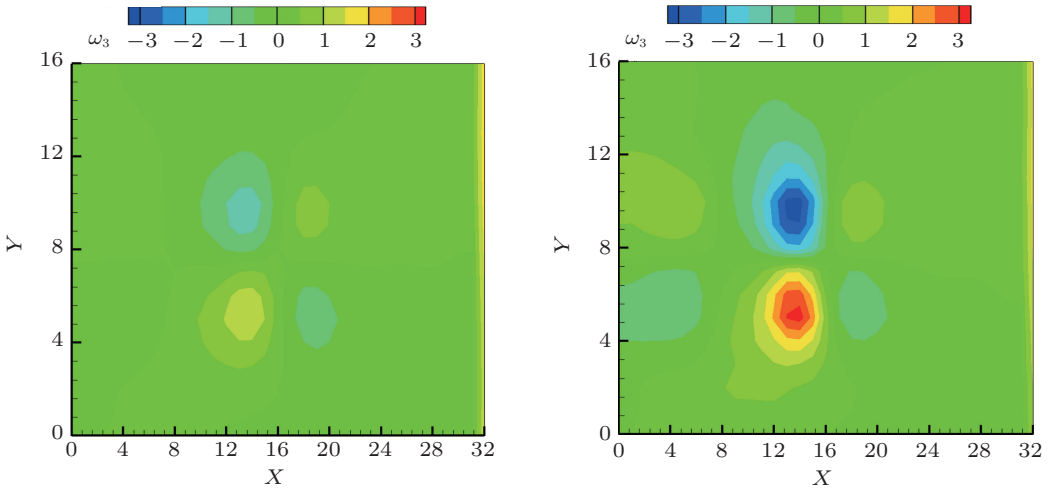

(a) PAM (b) Water

Fig. 4. Contours of spanwise vorticity during ejection.

of the Reynolds stress has considerably been inhibited and locates further from the wall in polymer additive solution. The reduction of Reynolds stress indicates the exchange of momentum weakens, and the turbulent fluctuations are suppressed because the viscoelasticity of the polymer. In the outer region of the flow, the magnitude of normalized Reynolds stress in the water is close to that in the solution. The different behavior of polymers in different regions suggests that the solution mainly suppresses the coherent motions in turbulent flow by damping the bursts of coherent structures. Meanwhile, this also confirms that coherent structures' bursting is the main mechanism for the maintenance, evolution and development of the turbulence.

The original velocity fluctuations of the solution and water flows are both decomposed into multi-scale components by local spatial averaged velocity structure function. As the maximum energy scale, only the fourth scale will be analyzed below. Its spatial scale corresponds to 16 grids, i.e., 9.078 mm. Then the spatial topologies of coherent structures in a detection area of 16×32 grids are obtained by the new mu-level criterion. The detecting center is set at $y^+ = 122$.

Figure 3 respectively presents the contours of streamwise fluctuating velocity in the solution and water flow during ejection at the fourth scale. In the two figures, the water follows from left to right. Obviously, surrounded with the high-speed fluid, the low-speed fluid ejects off the wall. Since the wall-normal velocity fluctuations are almost one order of magnitude smaller than the streamwise ones, the vectors seem to be a little parallel to the wall. Efficiently identifying the ejection of coherent structures indicates the accuracy of the new detecting criterion. In Fig. 3(a), the distribution of streamwise velocity fluctuations appears more regular. It is indicated that the polymers suppress

the fluid motion in the turbulent boundary layer.

Figure 4 shows the spanwise vorticity component with and without polymer solution during ejection at the same Reynolds number. The two figures resemble each other in shape, while they have a great difference in the magnitude. As shown in these figures, a strong vortex with positive vorticity caused by low velocity fluid ejection is below the center of ejection. A vortex with negative vorticity appears above the positive vorticity by inducing effect. Another pair of counter-rotating vortexes is also generated by induced downstream, and their values are a little lower than the main vortex. It is obviously that in both figures there are antisymmetric structures, whose appearance is the universal feature of turbulent flow regeneration and sustaining. Compared with the water case, the magnitude values of vorticity decrease in the polymer solution. Due to the viscoelastic property of polymers, the rotating motions are suppressed in the solution.

In this study, TRPIV was performed to investigate the spatial topological character of coherent structures near the wall in the turbulent channel flow of polymer additive solution. From the Reynolds stress profiles, the Reynolds stress in the solution greatly reduces, which reflects that the exchange of momentum weakens due to the polymers. The solution suppresses the turbulent motion by weakening the burst of coherent structures. The spatial topologies of coherent structures have been extracted by using the new detection criteria. Although the polymer additive solution does not affect the spatial topological shape, the fluctuating velocity and velocity drastically decreases in the solution. Because of the polymer additives, the wall friction is reduced by suppressing coherent structures, the dominant structures in near-wall turbulence.

This work was supported by the National Natural Science Foundation of China (11272233), National Basic Research Program (973 Program) (2012CB720101) and 2012 opening subjects of The State Key Laboratory of Nonlinear Mechanics (LNM), Institute of Mechanics, Chinese Academy of Sciences.

1. B. A. Toms, Proceedings of the 1st International Congress on Rheology **2**, 135 (1948).
2. P. S. Virk, E. W. Merrill, H. S. Mickley, et al., J. Fluid Mech. **30**, 305 (1967).
3. M. M. Reischman and W. G. Tiederman, J. Fluid Mech. **70**, 369 (1975).
4. S. J. Kline, W. C. Reynolds, F. A. Schraub, et al., J. Fluid Mech. **30**, 741 (1967).
5. T. S. Luchik and W. G. Tiederman, J. Fluid Mech. **190**, 241 (1988).
6. M. Motozawa, S. Ishitsuka, K. Iwamoto, et al., Flow Turbulence Combust **88**, 121 (2012).
7. W. Liu and N. Jiang, Chin. Phys. Lett. **21**, 1989 (2004).
8. J. H. Liu, N. Jiang, Z. D. Wang, et al., Appl. Math. Mech. **26**, 495 (2005).
9. N. Jiang, W. Liu, J. H. Liu, et al., Science in China Series G-Physics Mechanics & Astronomy **51**, 857 (2008).
10. P. R. Kenis, Journal of Applied Polymer Science **15**, 607 (1971).
11. X. Fan and N. Jiang, Mechanics in Engineering **27**, 28 (2005).
12. M. D. Warholic, H. Massah, and T. J. Hanratty, Experiments in Fluids **27**, 461 (1999).